Nitro-substituted ruthenium(II) polypyridyl complexes synergise with ATR inhibitors to enhance replication stress in cancer cells

Yian Chee Gan[1,‡], Nur Aininie Yusoh[2,‡], Suet Lin Chia[3,4,5], Xiaohe Tian[2,*], Martin R. Gill[6,*] and Haslina Ahmad[1,4*]

[1]Department of Chemistry, Faculty of Science, Universiti Putra Malaysia, 43400 UPM Serdang, Selangor, Malaysia

[2]Department of Radiology, Huaxi MR Research Center (HMRRC), Institute of Radiology and Medical Imaging, West China Hospital of Sichuan University, Sichuan University, Chengdu, Sichuan, China

[3]Department of Microbiology, Faculty of Biotechnology and Biomolecular Science, Universiti Putra Malaysia, 43400 UPM Serdang, Selangor, Malaysia

[4]UPM-MAKNA Cancer Research Laboratory, Institute of Bioscience, Universiti Putra Malaysia, 43400 UPM Serdang, Selangor, Malaysia

[5]Malaysia Genome and Vaccine Institute, National Institutes of Biotechnology Malaysia, Jalan Bangi, 43000 Kajang, Malaysia

[6]Department of Chemistry, Faculty of Science and Engineering, Swansea University, Swansea, UK

Email: xiaohe.t@wchscu.cn, m.r.gill@swansea.ac.uk and haslina_ahmad@upm.edu.my

[‡]These authors contributed equally to the work.

Supplementary Methods:

Singlet oxygen detection (SOSG)

Singlet oxygen generation was assessed using SOSG probe. SOSG (5 µM) was prepared in PBS and mixed with complexes **1**-**3** (10 µM). Fluorescence was recorded on a microplate reader at λ_{ex} = 504 nm and λ_{em} = 525 nm at 0-30 min. Background fluorescence from SOSG-only and buffer-only controls was subtracted. A singlet oxygen-generating control (rose bengal, 10 µM)

was included under identical conditions with white-light irradiation to confirm probe responsiveness.

Supplementary Tables:

Table S1. Fitted biexponential lifetime parameters (τ_1, τ_2) for complexes **1**-**3** recorded in acetonitrile (λ_{ex} = 450 nm).

Compound	$\lambda_{ex.}$ (max.) (nm)	$\lambda_{em.}$ (max.) (nm)	τ_1 /ns (%)	τ_2 /ns (%)
1	446	605	171 (82)	607 (18)
2	450	605	191 (83)	614 (17)
3	456	600	160 (76)	519 (24)

Table S2. DNA binding affinity parameters of complexes **1**-**3** with CT-DNA, determined from UV-Visible titration experiments. K_b = DNA binding constant.

Compound	DNA K_b (M^{-1})
$[Ru(dppz)_2(o\text{-NPIP})]^{2+}$ **(1)**	8.6×10^6
$[Ru(dppz)_2(m\text{-NPIP})]^{2+}$ **(2)**	1.0×10^6
$[Ru(dppz)_2(p\text{-NPIP})]^{2+}$ **(3)**	2.5×10^6

Table S3. Stern-Volmer quenching parameters obtained from EB-DNA competitive fluorescence titration of the Ru(II) complexes. The Stern-Volmer constants (K_{SV}) were derived from the slope of the linear plots of $I_o/I = 1 + K_{SV}[Q]$, and the correlation coefficients (R^2) represent the goodness of fit. All complexes exhibited linear quenching behaviour, with efficiencies following the order **3** > **2** > **1**.

Compound	DNA/EB ratio	K_{SV} ($\times 10^5$ M^{-1})	R^2	Observation
1	4.6	1.52	0.991	Linear Stern-Volmer plot; moderate quenching efficiency
2	4.3	1.58	0.996	Linear Stern-Volmer plot; stronger quenching than RuO

3	4.9	2.11	0.989	Linear Stern-Volmer plot; most efficient EB displacement

Table S4. 72 h half-maximal inhibitory concentrations (IC_{50}) of complexes **1**-**3** and parent molecule Ru-PIP determined by MTT assay. Data are presented as mean ± SD.

Compound	72 h IC_{50} (μM)			
	MCF7	**A549**	**HeLa**	**MRC5**
1	37.72 ± 1.41	43.58 ± 0.73	40.72 ± 2.04	>100
2	42.27 ± 2.11	41.66 ± 0.67	43.76 ± 0.87	>100
3	37.42 ± 0.76	39.05 ± 1.42	43.49 ± 1.12	>100
Ru-PIP	28.04 ± 1.57	30.08 ± 0.24	41.56 ± 1.79	>100

Supplementary Figures:

A

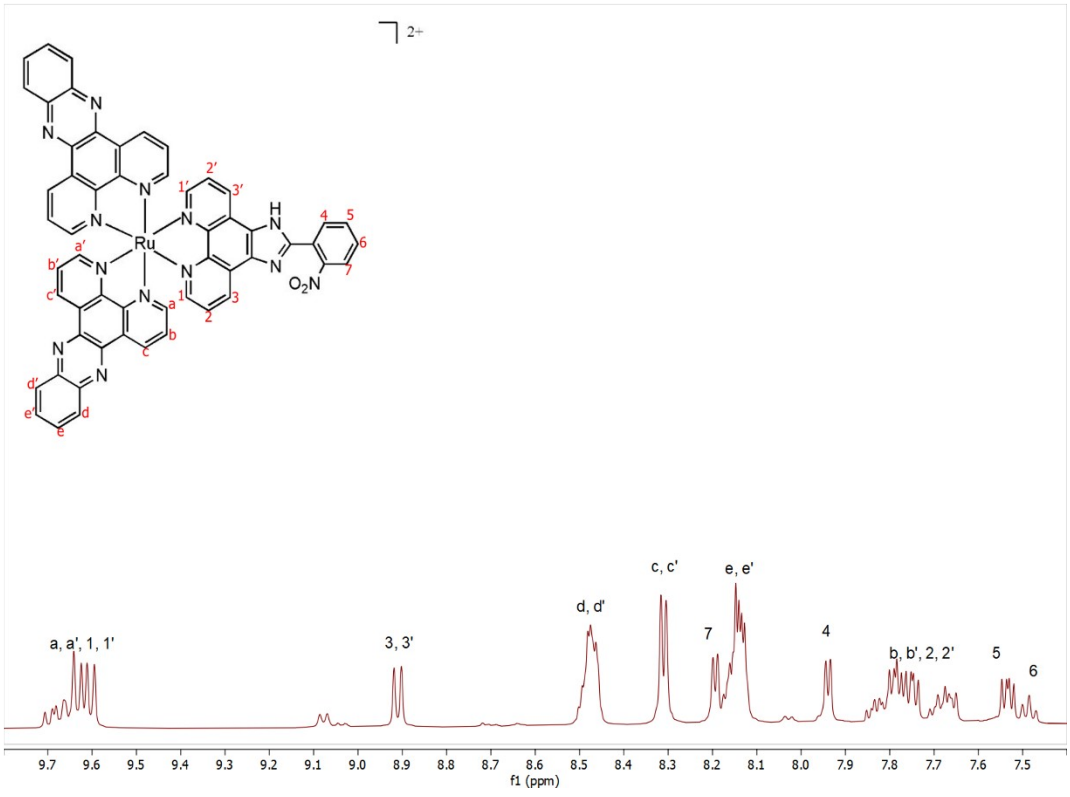

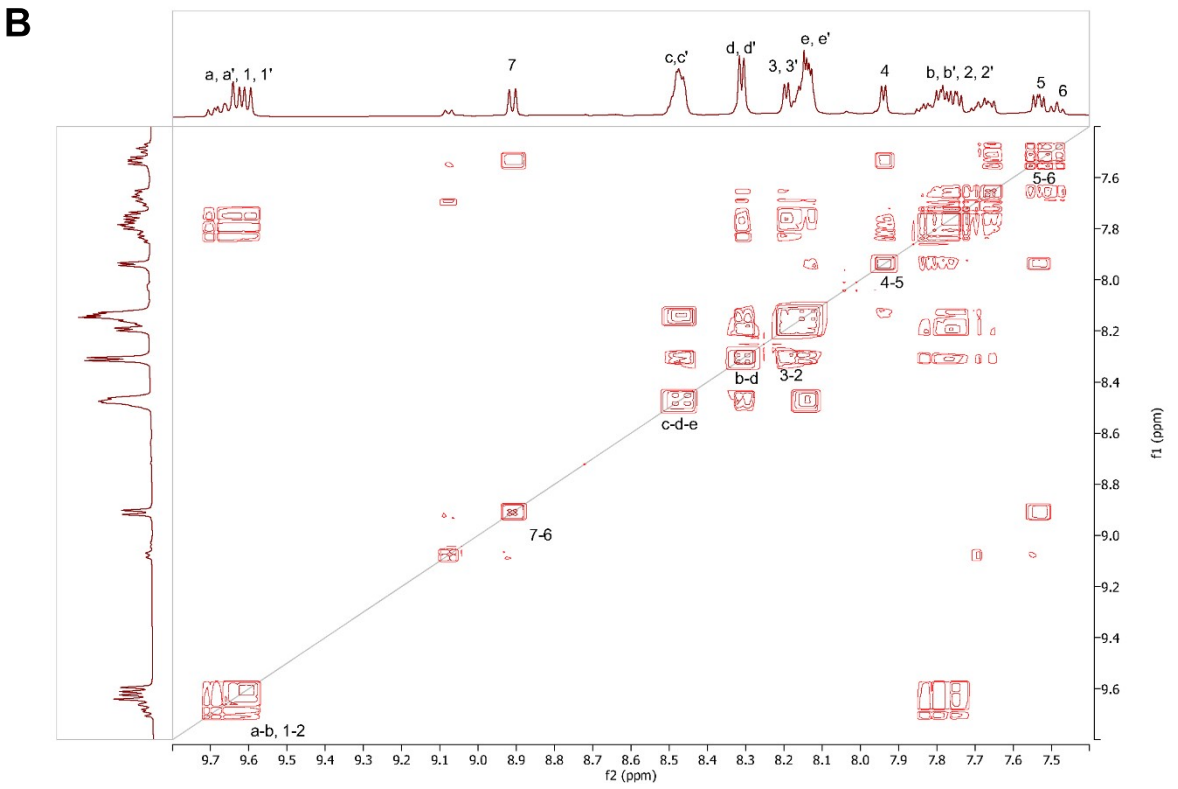

Figure S1. (A) ^{1}H NMR spectrum and (B) corresponding 2D ^{1}H-^{1}H COSY spectrum of **1** recorded in CD_3CN on a 500 MHz NMR spectrometer at 298 K.

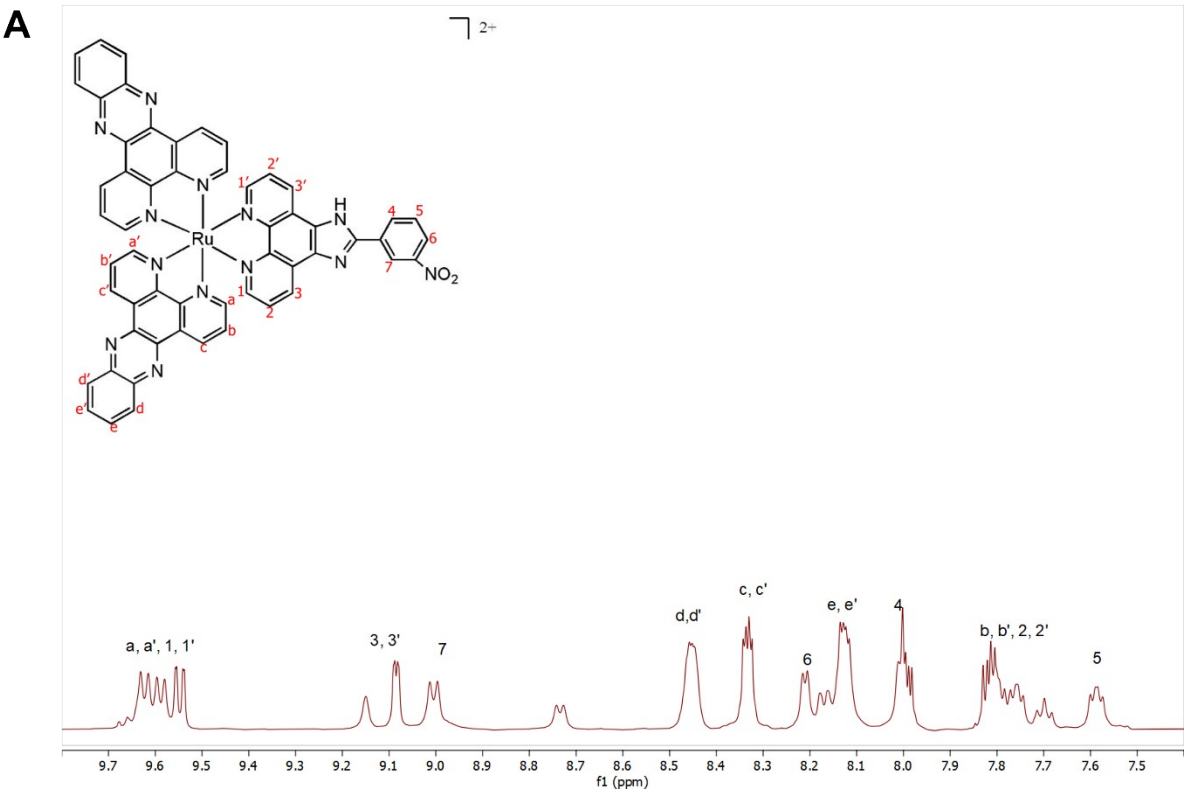

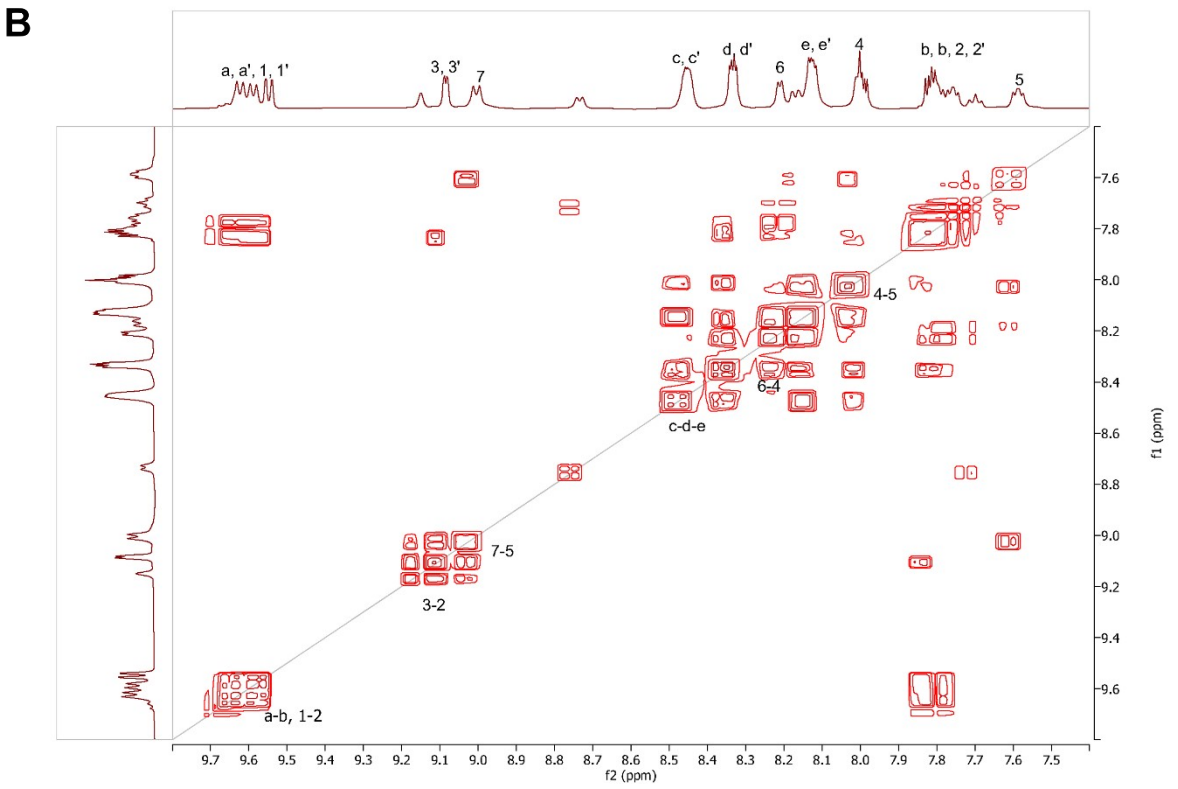

Figure S2. (A) ^{1}H NMR spectrum and (B) corresponding 2D ^{1}H-^{1}H COSY spectrum of **2** recorded in CD_3CN on a 500 MHz NMR spectrometer at 298 K.

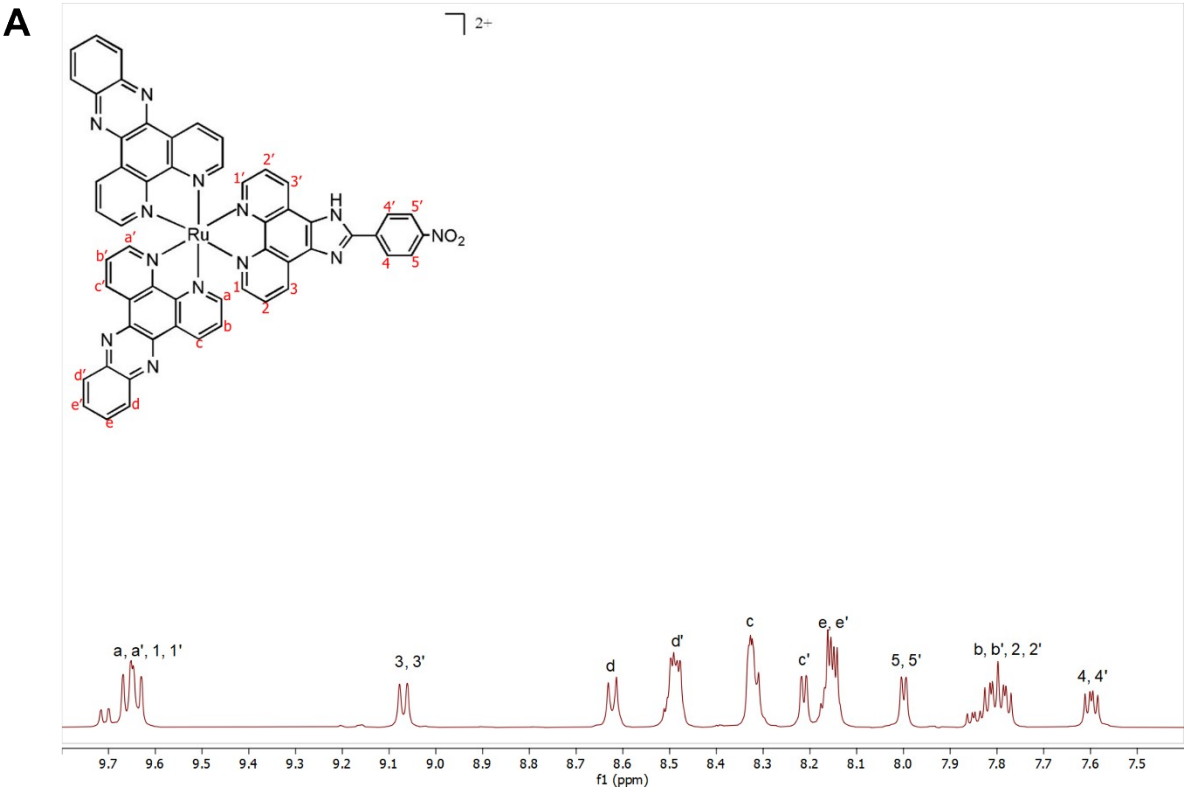

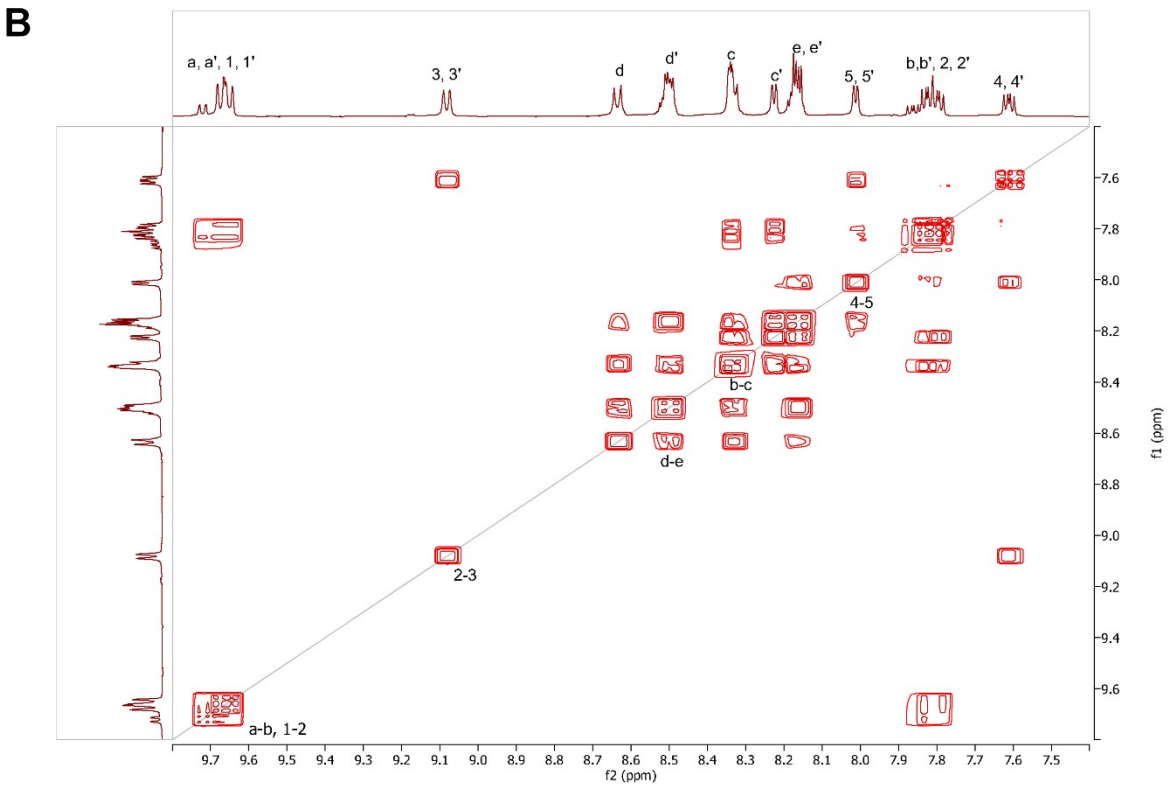

Figure S3. (A) ^{1}H NMR spectrum and (B) corresponding 2D ^{1}H-^{1}H COSY spectrum of **3** recorded in CD_3CN on a 500 MHz NMR spectrometer at 298 K.

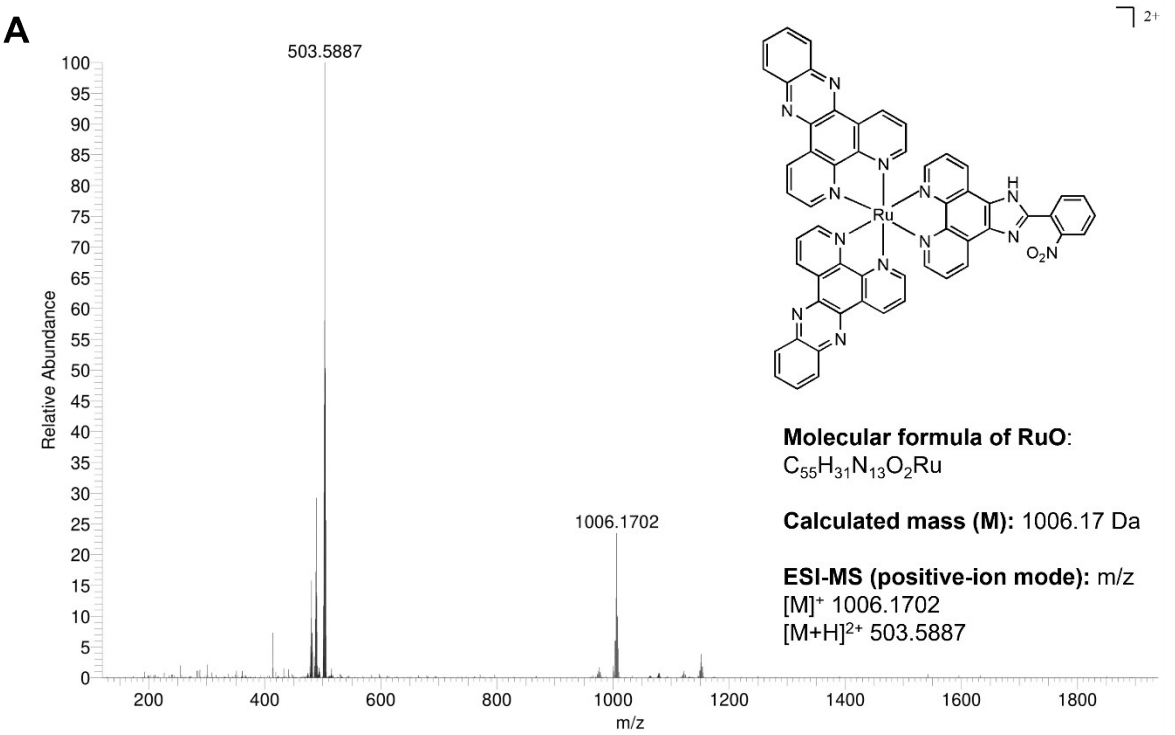

Figure S4. ESI-MS spectrum of **1.**

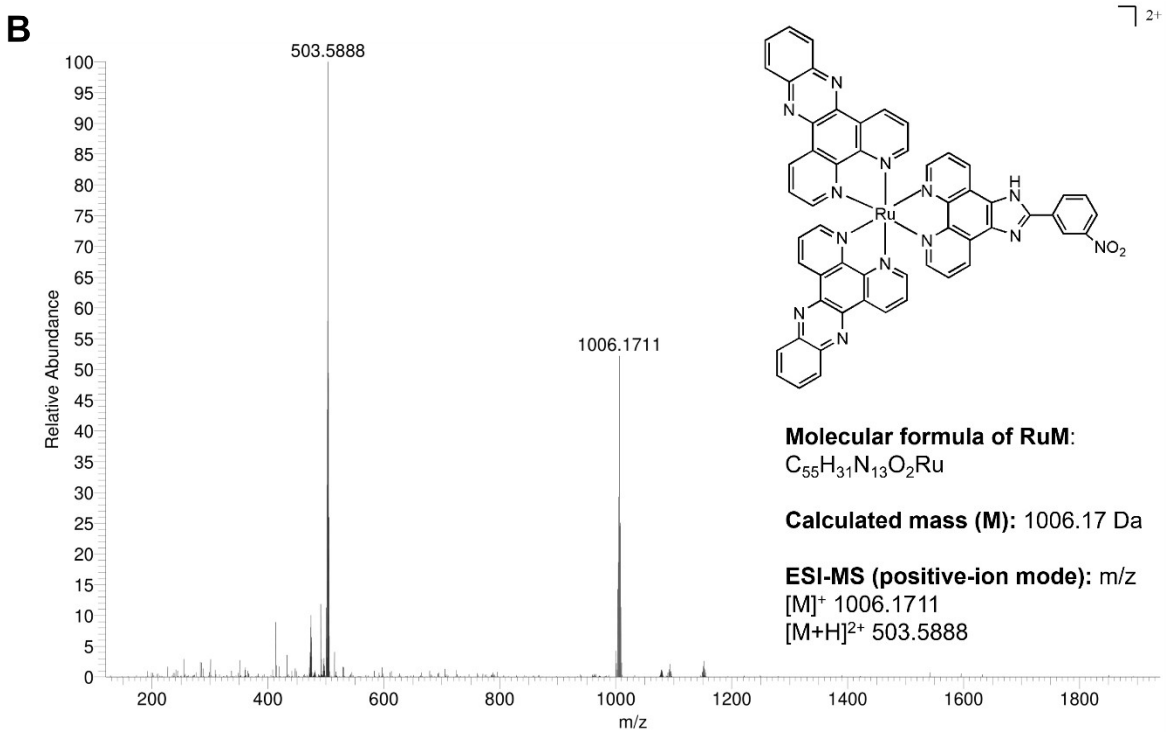

Figure S5. ESI-MS spectrum of **2**.

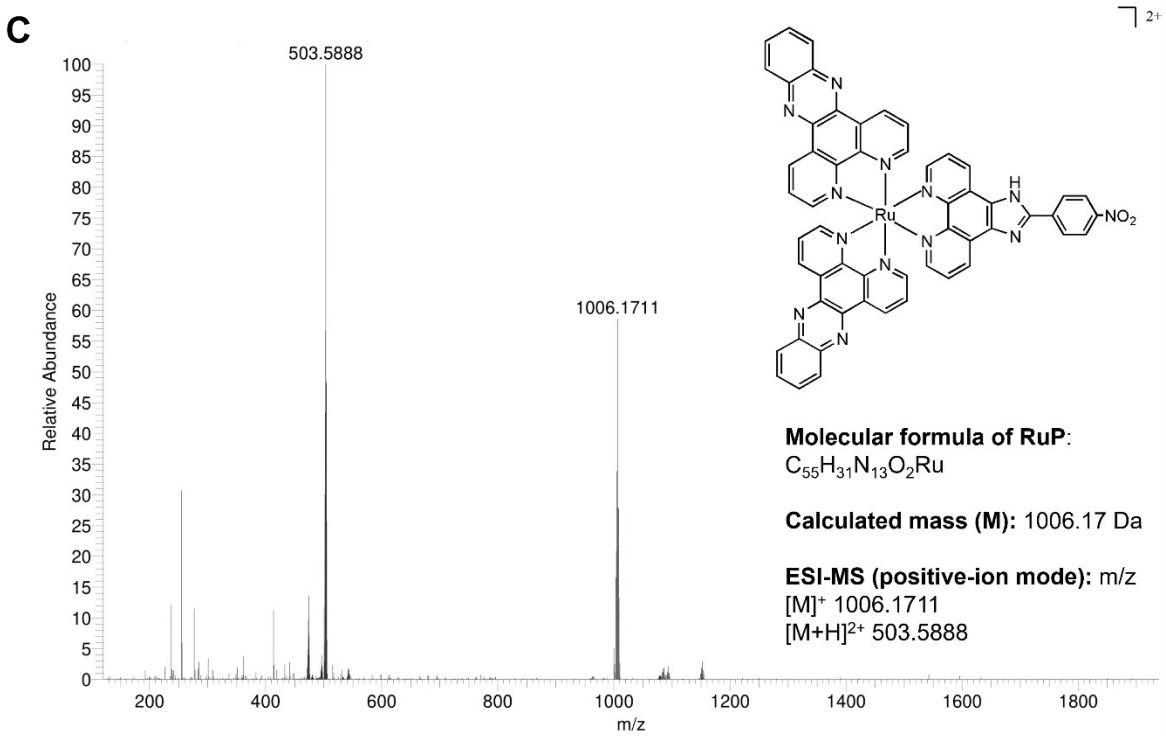

Figure S6. ESI-MS spectrum of **3**.

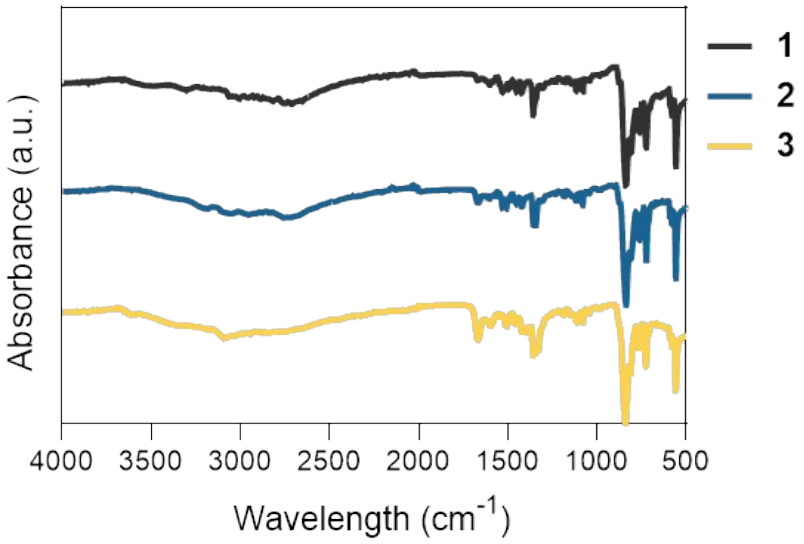

Figure S7. FT-IR spectra of **1-3.**

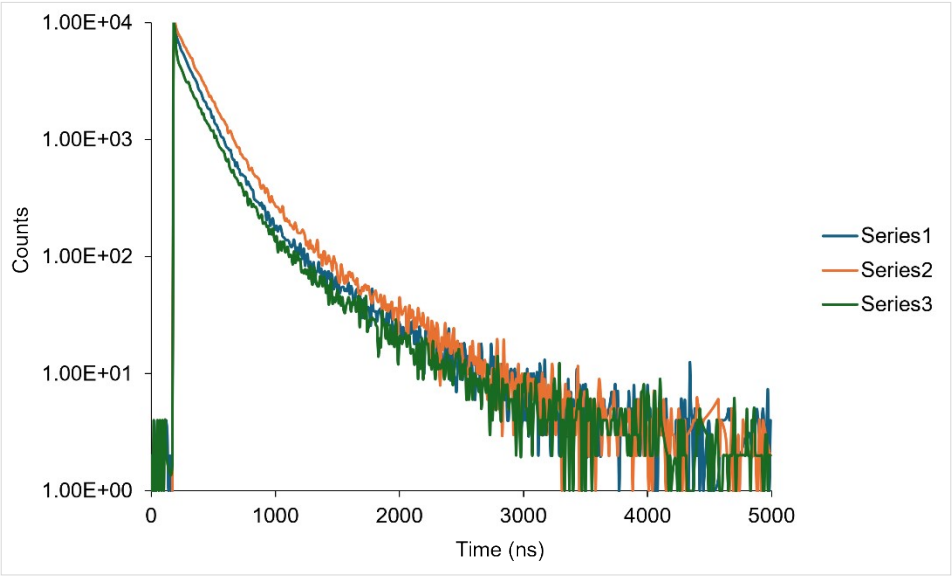

Figure S8. Lifetime decay profiles of complexes **1**-**3** recorded in acetonitrile (λ_{ex} = 450 nm). All complexes exhibit biexponential ^{3}MLCT decay behaviour.

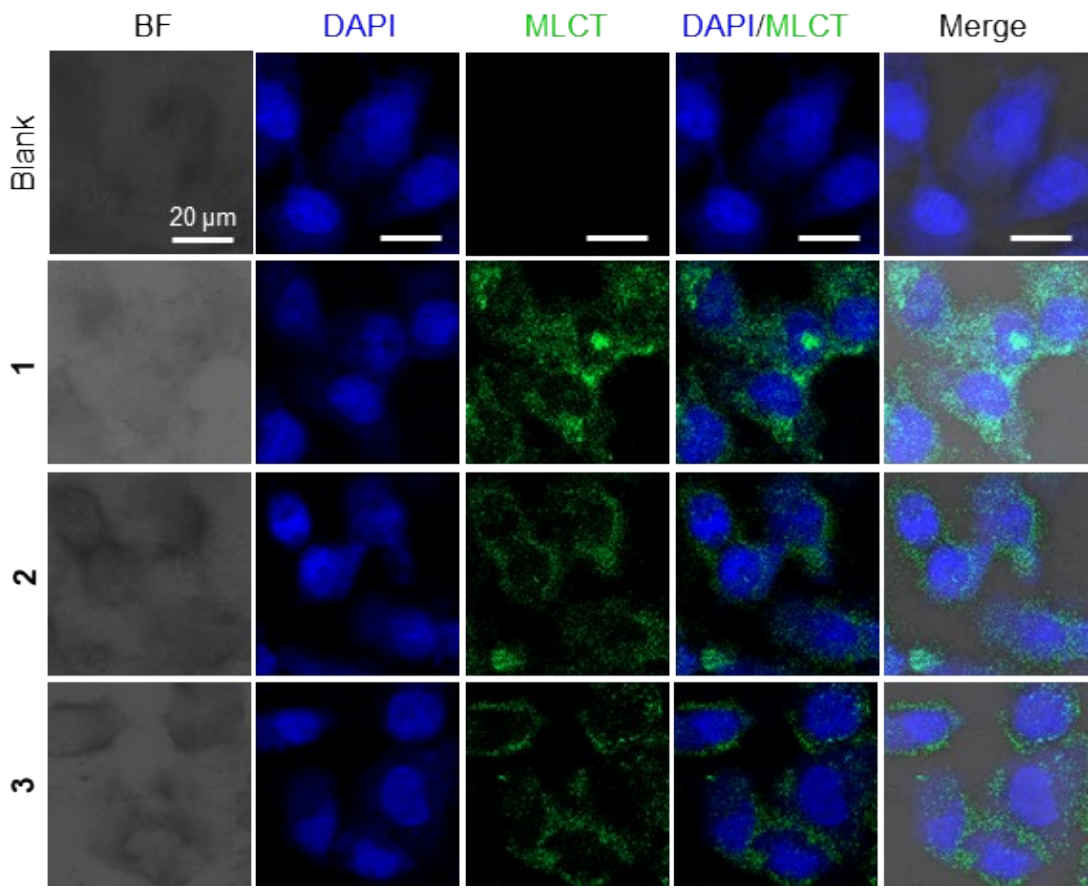

Figure S9. Confocal fluorescence images of HeLa cells treated with complexes **1-3** (100 μM, 1 h). Complexes were excited at 488 nm, and emission was collected between 600-750 nm. Nuclei were counterstained with DAPI. Scale bars = 20 μm.

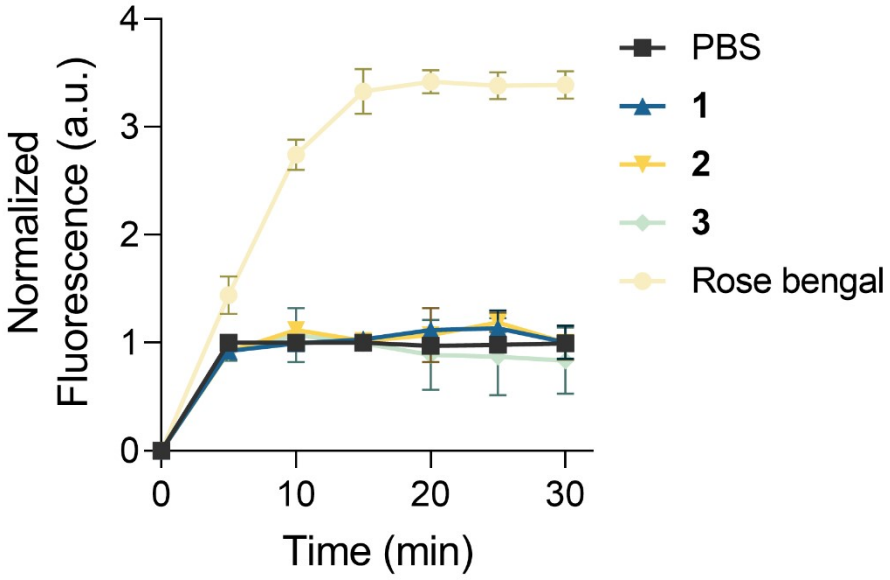

Figure S10. Singlet oxygen ($^1O_2$) generation using SOSG.

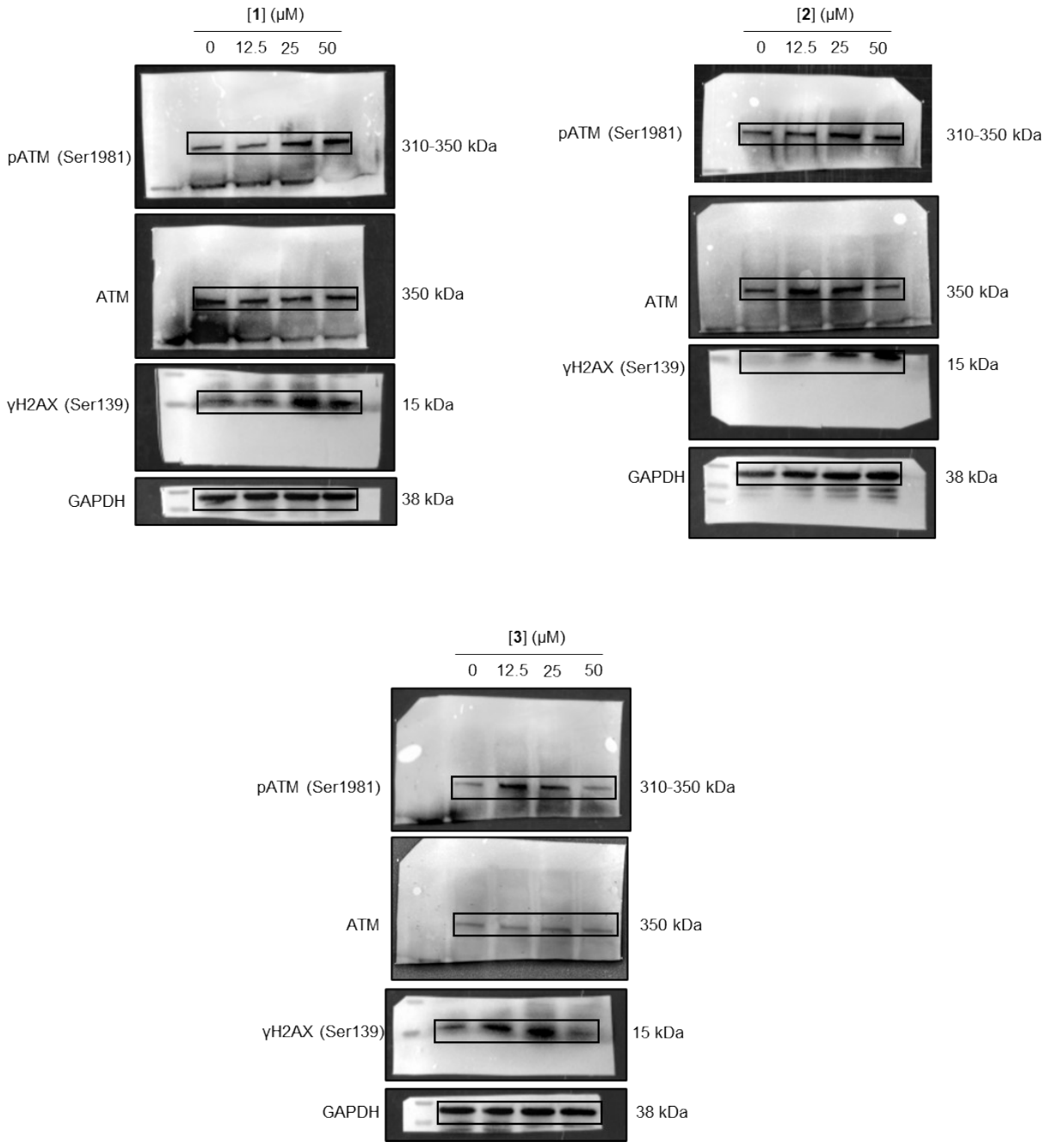

Figure S11. Uncropped blots for Fig. 4c.

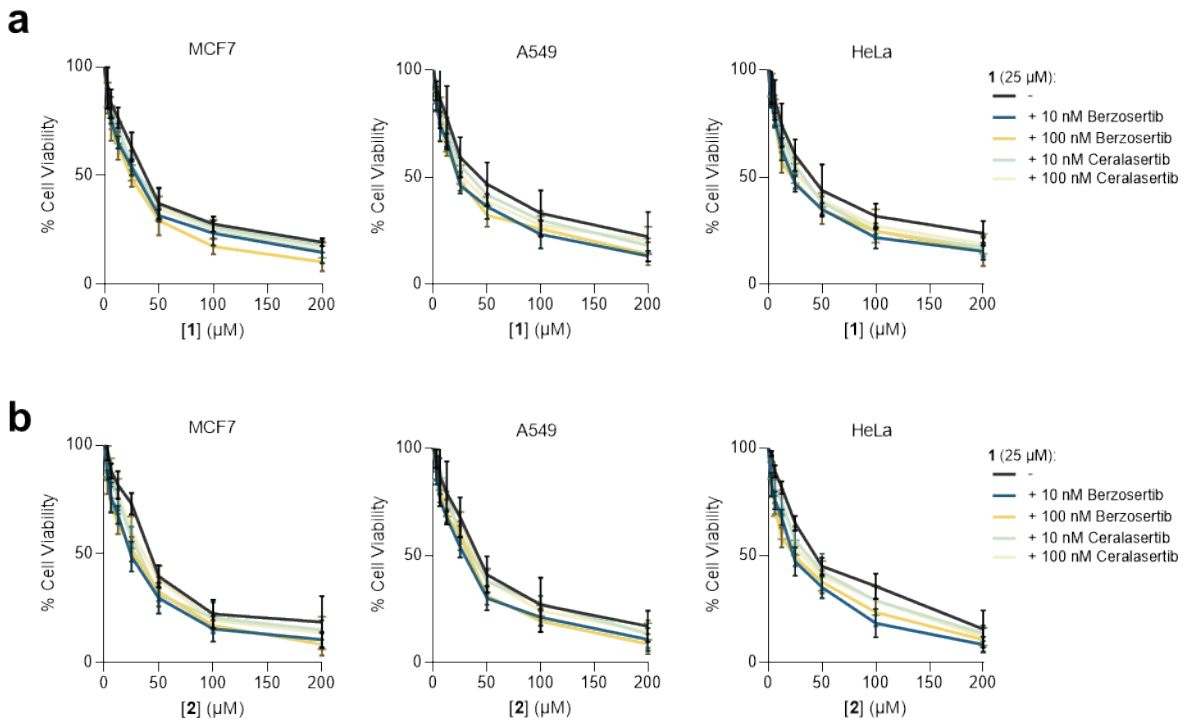

Figure S12. Cell viability of MCF7, A549 and HeLa cells treated with complexes (a) **1** and (b) **2** in combination with ceralasertib (0.01 μM) or berzosertib (0.01 μM) for 72 h, assessed by MTT assay. Data represent mean ± SD from three independent experiments.

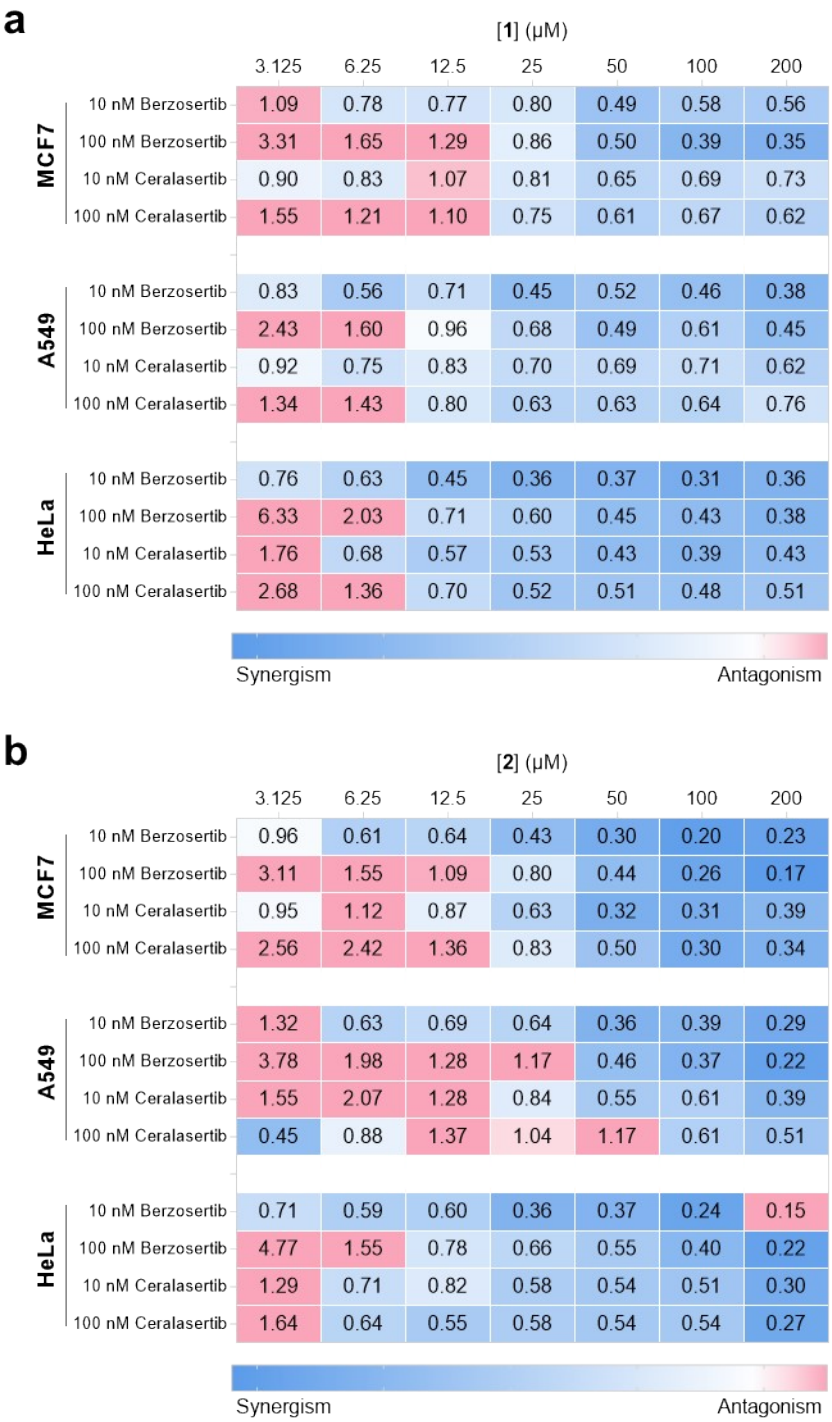

Figure S13. Combination indices for complexes (a) **1** and (b) **2** in combination with ATRi calculated using the Chou-Talalay method. CI < 1 = synergism and CI >1 antagonism.

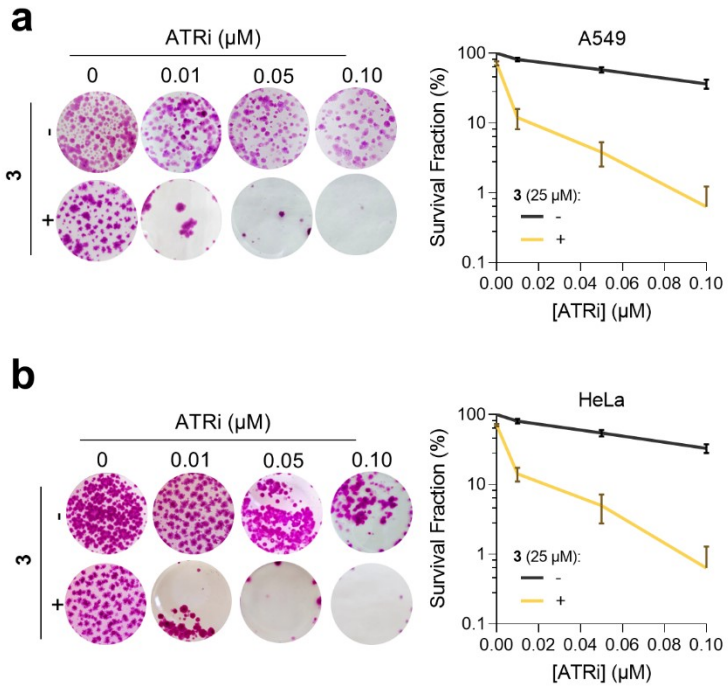

Figure S14. Clonogenic survival of A549 and HeLa cells after treated with concentration gradient of ATRi in the presence and absence of **3** (25 μM). Data represent mean ± SD from three independent experiments.

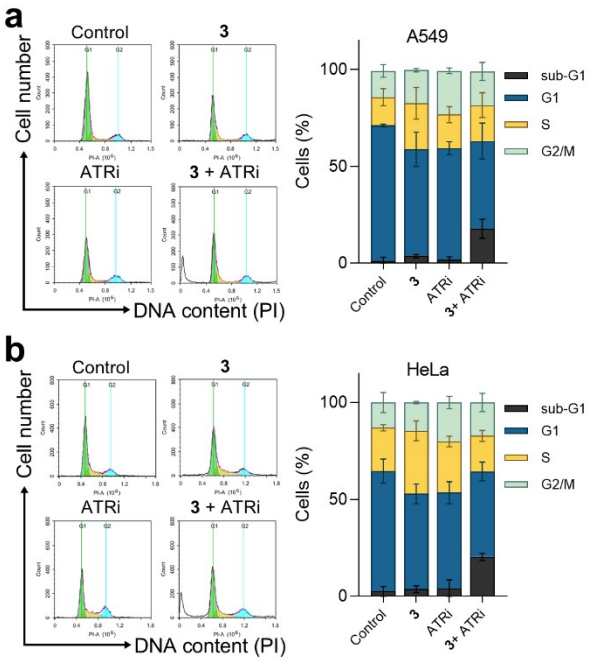

Figure S15. Cell-cycle distribution of (a) A549 and (b) HeLa cells treated for 72 h with complex **3** (25 μM) in combination with ATRi berzosertib (0.01 μM). Data represent mean ± SD from three independent experiments.

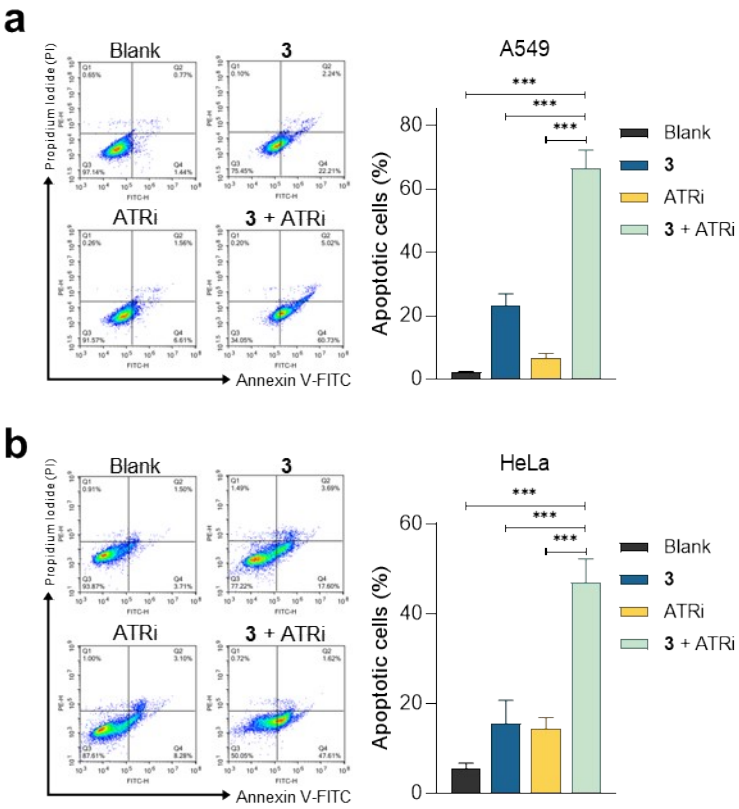

Figure S16. Annexin V-FITC/PI flow cytometry analysis of apoptosis in (a) A549 and (b) HeLa cells treated with complex **3** (25 μM), berzosertib (0.01 μM), or the combination for 72 h. Data represent mean ± SD from three independent experiments. ***P < 0.001 by ANOVA.

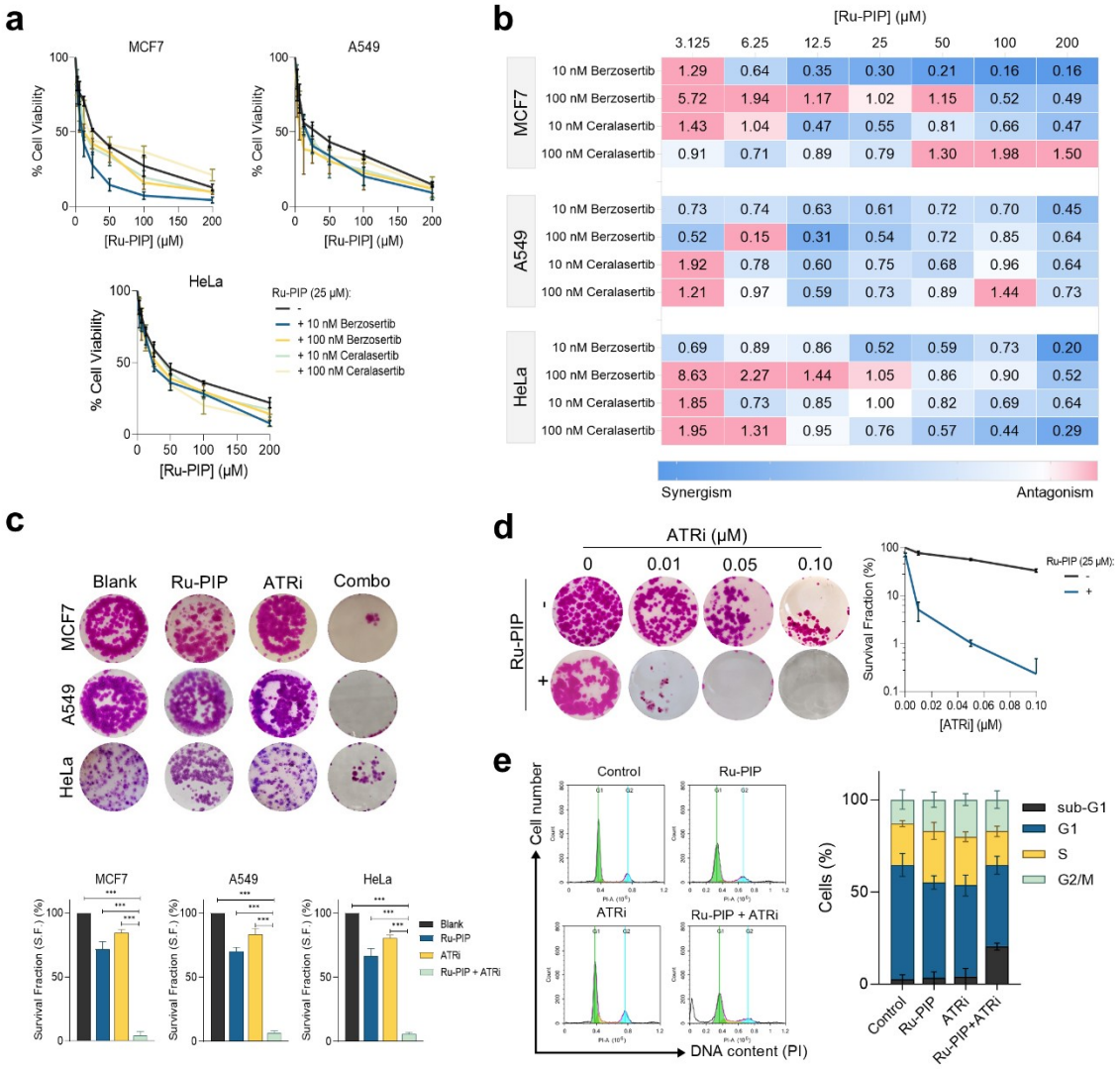

Fig. S17. Synergistic activity of Ru-PIP with ATR inhibitors. a) Cell viability of MCF7, A549 and HeLa cells treated with Ru-PIP in combination with ceralasertib (0.01 μM) or berzosertib (0.01 μM) for 72 h, assessed by MTT assay. Data represent mean ± SD from three independent experiments. b) Combination indices calculated using the Chou-Talalay method. CI < 1 = synergism and CI > 1 antagonism. c) Clonogenic survival of cells treated for 72 h with Ru-PIP (25 μM) in combination with berzosertib (0.01 μM). d) Clonogenic survival of MCF7 cells after treatment with a concentration gradient of ATR inhibitor in the presence and absence of Ru-PIP (25 μM). e) Cell-cycle distribution of MCF7 cells treated for 72 h with Ru-PIP (25 μM) in combination with berzosertib (0.01 μM). Data represent mean ± SD from three independent experiments. ***P < 0.001 by ANOVA.

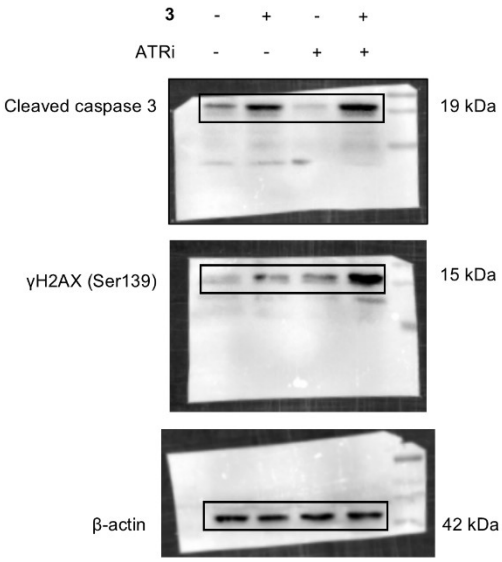

Figure S18. Uncropped blots for Fig. 6c.

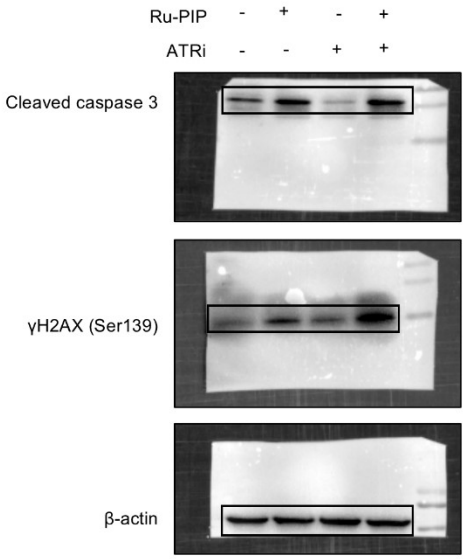

Figure S19. Uncropped blots for Fig. S18c.